



Hu, Z., Timmons, T., Stamat, L. and McInnes, C. (2020) Development of a 10g femto-satellite with active attitude control. *Journal of the British Interplanetary Society*, 73(5), pp. 163-169.

There may be differences between this version and the published version. You are advised to consult the publisher's version if you wish to cite from it.

<http://eprints.gla.ac.uk/221823/>

Deposited on 22 November 2019

Enlighten – Research publications by members of the University of Glasgow
<http://eprints.gla.ac.uk>

Development of a 10g Femto-satellite with Active Attitude Control

Zhongxu Hu

James Watt School of Engineering, University of Glasgow

Zhongxu.hu@glasgow.ac.uk

Thomas Timmons

James Watt School of Engineering, University of Glasgow

t.timmons.1@research.gla.ac.uk

Liviu Stamat

James Watt School of Engineering, University of Glasgow

l.stamat.1@research.gla.ac.uk

Colin McInnes

James Watt School of Engineering, University of Glasgow

colin.mcinnnes@glasgow.ac.uk

ABSTRACT

This paper describes the initial design of a Femto-satellite with active attitude control. It has a structure with a matchbox form factor, measures 3.5 x 3.5 x 0.5cm, and uses three miniaturized orthogonal magnetorquers as actuators for attitude control. It also features short range RF communication at 868 MHz for demonstrating satellite networking and swarming around a CubeSat as a host. Preliminary test results obtained from a prototype device weighing 10g are given, including IMU based attitude determination, miniaturized magnetorquers, a custom-built Helmholtz coil system, active attitude control and RF communications.

KEYWORDS: Femto-satellite, miniature magnetorquers, active attitude control

1 INTRODUCTION

Rapid progress in sensor/actuator miniaturization based on MEMS technology^[1], on-board computing and efficient energy conversion and storage, has enabled a scaling-down in spacecraft size from large multi-ton geostationary communication platforms, to 100 kg class small satellites and the recent rapid growth of CubeSats. In recent years, there are growing interests in femto-satellites with a characteristic mass between 10g to 100g, which maybe mass produced and deployed as a cluster or a swarm of satellites.

A number of research groups are developing femto-satellite platforms, for example, SpaceChips or “smart dust”^{[2][3]}, PCBSat^[4], RyeFemsat^[5], WikiSat^[6] and Sprite^{[7][8]}. These developments are mainly motivated by significantly reduced launch costs, and the potential for novel distributed applications based on clusters and swarming of large numbers of devices^[9]. However, the key problem with femto-satellites currently preventing them from practical commercial applications are their limited payload capacities, the lack of power required to operate payloads such as long-range high-power RF links and camera systems, and the lack of attitude control. As a result, most of the reported femto-satellite projects are passive devices, which were used only to demonstrate in-orbit communication with very low data rates or as RF beacons^[7]. Therefore, the development and demonstration of a femto-satellite with the capability

Copyright © 2019 by Z. Hu, T. Timmons, L. Stamat, and C. McInnes. Published by the British Interplanetary Society with permission.

to actively adjust its attitude, for example to maximize solar power, and to transfer sensor data at a high rate represents significant progress.

Through our programme of research, we are developing a femto-satellite, with dimensions $3.3 \times 3.3 \times 0.5$ cm. A prototype of an initial device weighs 9.9 grams. Importantly, the device has active 3-axis attitude control using miniaturized orthogonal magnetorquers driven by MEMS gyroscopes and a 3-axis magnetometer. The system is designed around a TI's cc430 system on chip (SoC) device with built-in low power RF communications, which transmits attitude data and commands between the femto-satellite and a CubeSat as a host. The host CubeSat is proposed to serve as the femto-satellite deployer and communication relay.

This paper will present the development of an initial design and a laboratory prototype device which features short-range high data rate RF communications, efficient solar cells and embedded power control for in-orbit operations. Building on this initial device, we plan a number of devices which will be fabricated to demonstrate laboratory-scale networking and localization capabilities based on the RF received signal strength indicator (RSSI).

Following a description of the laboratory-scale development of the current device in section 2, initial results on attitude determination based on explicit complementary filter (ECF) sensor fusion is presented in section 3, a simple implementation of attitude control based on the linearized system dynamics is described in section 4, and RF communication testing, magnetorquer testing and a custom-built Helmholtz coil system are described thereafter. Concepts for in-orbit demonstration will be provided using a CubeSat carrier along with the regulatory challenges posed by devices at such small length-scales. Finally, a number of potential applications will be reviewed including technology demonstration, massively parallel sensing for space science, distributed antennae and deep space applications.

2 SYSTEM DESCRIPTION

In most reported femto-satellite projects, data communication is carried out directly between the satellite and a ground station. Limited by RF power, the data rate is kept low so that long range data transfer is possible. This project is configured around a CubeSat as a carrier/deployer, and also as a communication hub and relay, as shown in figure 1.

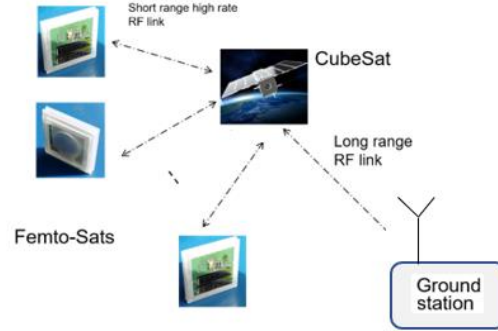


Figure 1. Swarm of femto-satellites based around a CubeSat as a communications hub.

The system, as shown in figure 2, is designed around a TI SoC chip, cc430F5137, with built-in RF functionality. The SoC accesses a 9 axes IMU via an SPI interface, and outputs three channels of PWM signals to control three H bridges, which drive the three orthogonal magnetorquers separately. The SoC transmits /receives RF data using a monopole antenna through a matching circuit. The electrical power system consists of a DC-DC converter, and power control, for example if the voltage is low, the RF channel and magnetorquers can be switched off.

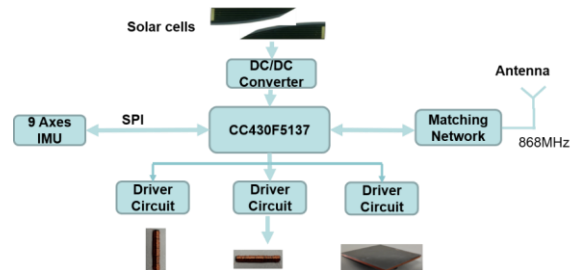


Figure 2. Block diagram of femto-satellite design around a TI cc430 SoC.

Figure 3 shows the assembled PCB, and the 3D printed matchbox case where the air coil magnetorquer is wound, and the coin cell battery is mounted.

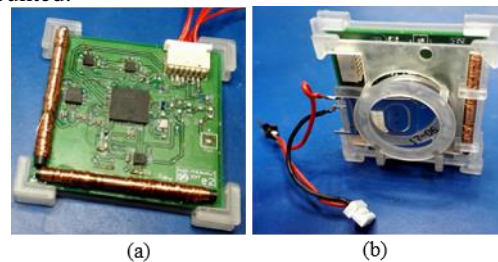


Figure 3. (a), assembled PCB, (b), powered by solar cells and a coin cell battery.

3 ECF BASED ATTITUDE DETERMINATION

Attitude determination is essential for active attitude control. The femto-satellite device features a low cost 9 axis IMU, MPU9250, made by TDK InvenSense. The attitude is estimated from the magnetometer and gyroscope measurements via a sensor fusion algorithm. The accelerometer which measures the local gravity can't be used in the orbital environment. There are popular algorithms for sensor fusion, such as the Kalman filter, gradient descent optimization, and the explicit complementary filter (ECF) with a close-loop feedback configuration. The ECF is implemented and tested in this initial development of the femto-satellite ADCS.

3.1 Magnetometer calibration

The magnetometer can't be used without calibration due to its large offset and scale factor error, which causes large attitude errors. A simple calibration process is based on the fact that the response surface of an ideal magnetometer to the Earth's magnetic field vector should be a sphere centred at the 3D origin. In figure 4, the red, green and blue dots respectively represent plot of magnetometer readings M_x vs M_y , M_x vs M_z and M_y vs M_z . It shows the raw data from the magnetometer before calibration, and corrected sensor data after the offset and scale factor errors have been removed.

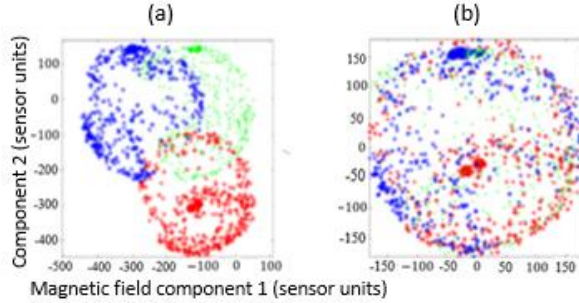


Figure 4. Removal of offset and scale factor errors of the magnetometer. (a) raw data, (b) corrected.

3.2 ECF

The block diagram of the explicit complimentary filter (ECF) is shown in figure 5, where $\bar{\mathbf{M}}$ is the earth's magnetic field vector measured in the satellite's frame by the on-board magnetometer, \mathbf{M}_0 is the known earth's magnetic field vector in the Earth's inertial frame, and $\hat{\mathbf{M}}$ is an estimation of the Earth's magnetic field vector in the satellite's frame via rotation transformation by the orientation

quaternion \mathbf{q} . Ideally, if the attitude quaternion is correct and precise, then the estimation $\hat{\mathbf{M}}$ should match the measurements $\bar{\mathbf{M}}$ perfectly. The ECF sensor fusion algorithm compares the two vectors $\bar{\mathbf{M}}$ and $\hat{\mathbf{M}}$, and calculates the attitude error by the cross product $\mathbf{e} = \bar{\mathbf{M}} \times \hat{\mathbf{M}}$, which is used to adjust the attitude quaternion \mathbf{q} by proportional and integral (PI) control. The angular rate $\boldsymbol{\omega}$ from the gyroscope sensor serves as feedforward control to improve the bandwidth of attitude determination.

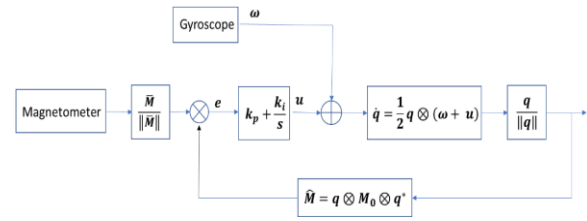


Figure 5. Block diagram of ECF using a 3-axes magnetometer and a 3-axes gyroscope.

3.3 Effect of Magnetorquers

Three orthogonal magnetorquers are used as actuators for the attitude control, as will be described later in section 4. When activated, these magnetorquers generate magnetic dipoles, which interact with the Earth's magnetic field to produce control torques on the femto-satellite's axes. Constrained by the size of the femto-satellite, the magnetorquers are placed very close to the IMU sensor, resulting in an extra magnetic field proportional to the drive currents being added to the output of the magnetometer. This will inevitably affect the accuracy of attitude estimation or stop it working completely. Figure 6 shows the effects of activated magnetorquers on the measurements of the local magnetic field. This effect has to be removed to ensure correct attitude determination using sensor fusion algorithms.

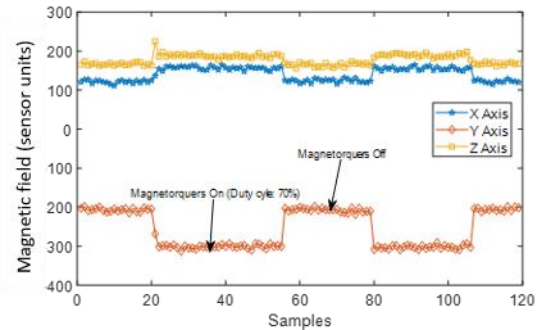


Figure 6. Activated magnetorquers add to local field.

The local distortion to the earth's magnetic field caused by the magnetorquers is avoided by switching off the magnetorquers at the H bridge drivers, and adding a delay before reading the magnetometer. The length of the delay depends on the inductance of the magnetorquers. Initial tests show a 5ms delay is enough to entirely eliminate the effects. Figure 7 is a screenshot of the visualization of the attitude estimation via the explicit complementary filter.

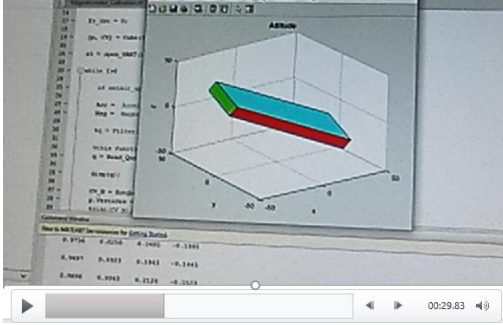


Figure 7. Visualization of attitude determination.

4 ATTITUDE CONTROL

After the attitude quaternion is estimated with the ECF as described in section 3, and the three axes rotation rates ω are readily available from the gyroscope sensor, simple attitude control is implemented. Figure 8 shows the block diagram of the “P2” attitude control based on the linearized satellite dynamics. The satellite attitude is described in quaternion form. The attitude error is calculated using quaternion multiplication between the desired attitude quaternion q_d and conjugate of the estimated attitude quaternion q_s^* :

$$q_e = q_d \otimes q_s^* \quad (1)$$

The attitude control torques are synthesized using the estimated attitude and rotation rates:

$$\tau = -k_p q_e - k_d \omega \quad (2)$$

Because the attitude control is based on a linearized dynamic model, where the Coriolis coupling between axes are neglected, this assumes the satellite body rotation rate is already low via an active de-tumbling control using the magnetorquers. This detumbling control algorithm is given by:

$$m = -k\dot{B}, \quad (3)$$

$$\tau = -k(\omega \times B) \times B \quad (4)$$

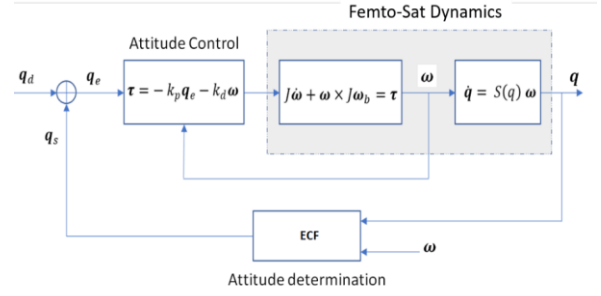


Figure 8. Attitude control based on linearized satellite dynamics.

5 RF COMMUNICATION TESTING

Half-duplex bi-directional RF communication has been tested successfully. The femto-satellite device sends attitude data in quaternion format, ACS status, and attitude control commands to the local ground station in the downlink direction. The ground station transmits the desired attitude, and ADS On/Off commands to the Femto-satellite in the uplink direction. At 0 dBm transmit power, the data stream speed for both directions is set at 38.4 kb/s, and reaches a distance of 70 meters. By fine tuning the matching circuit for the antenna and increasing the transmit power to the power limit of 14 dBm allowed by regulation, it is expected the communication distance can be increased to hundreds of meters at a relatively high data rate. The RF channel uses the frequency band at 868 MHz, which is exempt from licencing when the RF transmitting power is less than 14 dBm.

A useful feature the built-in RF module offers is the received signal strength indicator (RSSI), which may be used for relative localization of a cluster of femto-satellites. In the initial testing, when the transmit power is set at a low level of 0 dBm, as shown in figure 9, the RSSI value varies with distance between the femto-satellite and a receiver. A deviation of -40 dBm was recorded when the distance is extended to 50 meters inside a building.

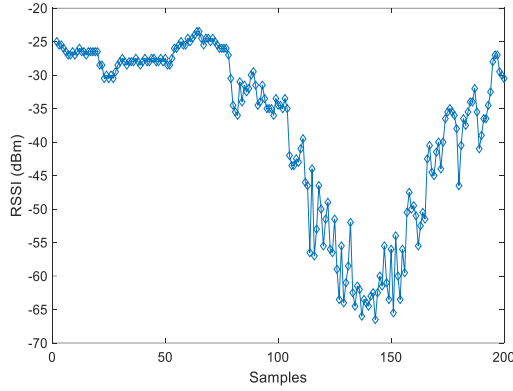


Figure 9. RSSI changes with distance between Femto-sat and a ground station.

6 ELECTRICAL POWER SYSTEM

The electrical power system is based around Linear Technology's step-up DC-DC converter controller LTC3105 with a very low start-up voltage of 0.25V, which stabilizes the output voltage at 3.3V even though the inputs from the solar cells fluctuate with the light source. Two 28% high efficiency solar cells, each measuring 26x8mm in size, are connected in parallel to provide electrical power. For each solar cell, the maximum output voltage is 2.6V, the maximum current is 14.5mA and the maximum output power is 34mW. A 65mAh coin button battery, and a number of high value capacitors are used as power storage and buffer.

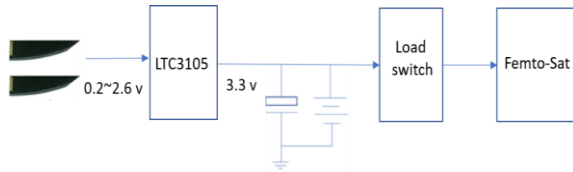


Figure 10. Solar cell based electrical power system.

The IMU sensor consumes a current of 4mA in sensing operation, the built-in RF module consumes 16mA in receive mode, and 34mA in transmit mode, though the RF module only transmits/receives for a very short period of time at a few hertz, and each of the three orthogonal magnetorquers consumes a maximum current of 30mA depending on the attitude error. The discharging current from the battery and capacitors may exceed the charging current from the solar cells, so that the voltage can never reach 3.3V. To overcome this problem, a load switch with hysteresis is placed between the EPS and the femto-

satellite. It is clear solar power is not enough to support continuous operation of the femto-satellite, so a new design with more solar cells is underway.

7 MINIATURIZED MAGNETORQUERS

The smallest commercial magnetorquer rod available off the shelf is made by ZARM Technik and measures 3.5 mm in diameter, and 55mm in length. It provides a maximum magnetic dipole moment of 0.1 Am². It is clear this magnetorquer does not fit the design size. Therefore, a custom designed and built torque rod and an air coil that provides the torque for the z-axis of the femto-satellite are used as actuators. The details of the magnetorquer design are listed in Table 1, where the ferrite core has a relative magnetic permeability of 2300. Figure 11 shows the three magnetorquers mounted on a prototype board simulating the PCB for lab testing.

Table 1. Magnetorquer design

	Ferrite-Core	Air-Core
Max. Moment [Am ²]	0.0025	0.0025
Number of Windings	300	70
Mass [g]	0.61	0.68
Dimensions [mm]	2.2 (D) X 30 (L)	35 x 35 x 1

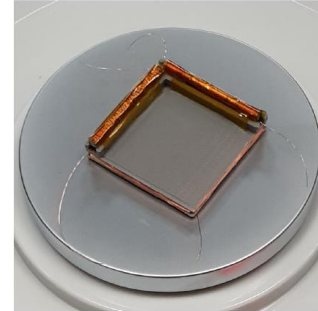


Figure 11. Three magnetorquers orthogonally mounted.

The magnetorquers are tested in a custom-built Helmholtz coil system. The maximum magnetic field the coil system can generate is 6 times that of the Earth's field in all three axes. The magnetorquer windings use enamelled wire of 0.1mm in diameter, which allows a maximum current of 30mA. A simple test using a suspension system is shown in figure 12. Test results show both the torque rods and air coil are able to swiftly rotate the PCB board.

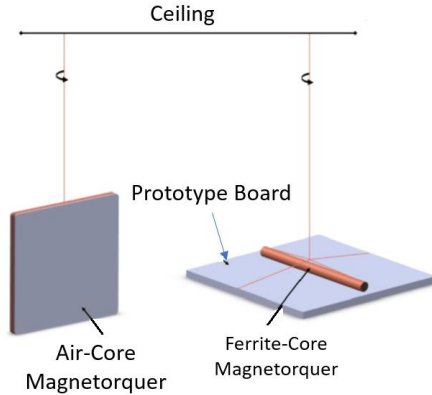


Figure. 12, Testing of magnetorquers with suspension system.

8 AIR BEARING AND 3D PRINTED TOP

The simple suspension system is able to test the attitude control in a single axis only. In order to test the attitude control of the femto-satellite for all the three axes, a spherical air bearing system is an ideal solution. However, the air bearing top of the available spherical bearing system has a mass of 216 grams, and mass moment of inertia of 0.14 gm^2 . These are about 200 times that of the femto-satellite device. To minimize the effects from the original air bearing top, a custom air bearing top weighing 6g is made using a high precision LSA 3D printer. Figure 13 shows the femto-satellite on top of the 3D printed air bearing top, and the test setup for the attitude control demonstration, including the air bearing system and the Helmholtz coil system.

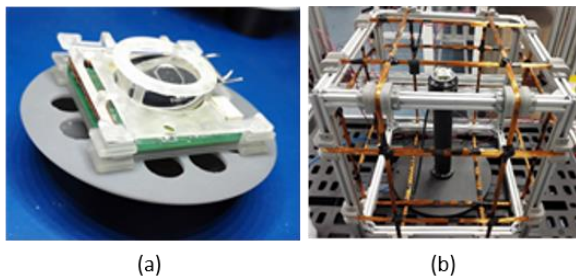


Figure. 13, 3D printed low mass & inertial air bearing top and the Helmholtz coil system.

9 FUTURE WORK

The major objectives of the initial design of the femto-satellite platform is to demonstrate the feasibility of attitude control using miniaturized magnetorquers, magnetometer-based attitude

determination under the influence of magnetorquers, the RF communication and the RSSI related localization. Initial test results show most of the objectives are feasible. However, it also shows the major limitations of the design: 1) solely magnetometer-based attitude determination has uncertainty in the direction perpendicular to the Earth's magnetic field; 2) very limited power from the two solar cells, which are unable to continuously operate the device; 3) more payloads, such as CMOS imager module, should be added to the platform without significantly increasing the size of the device.

In light of these considerations, a new design is underway. It will be based around a more powerful SoC chip, TI's cc1352. Major advantageous features over the initial design include: DSP instructions, a floating-point unit, sensor controller and dual RF band: sub-1GHz and 2.4GHz. The new design also has a sun sensor based on low cost quadrant photodiode from Optek / TT Electronics, which measures $7.5 \times 7.5 \times 1.5 \text{ mm}$. A 640×480 pixels CMOS imager with optics may be included, OVM7692, from OmniVision with a serial bus interface, which measures only $3.4 \times 2.9 \times 2.7 \text{ mm}$. More power is planned by adding more solar cells by a matchbox structure.

ACKNOWLEDGMENTS

This work was support by a Royal Academy of Engineering Chair in Emerging Technologies and an EPSRC DTP scholarship.

REFERENCES

1. Marsil A.C. Silva, Daduí C. Guerrieri, Angelo Cervone, Eberhard Gill, "A review of MEMS micropropulsion technologies for CubeSats and PocketQubes," *Acta Astronautica* 143 (2018) 234–243.
2. Keller, J. "Start-up to Develop Satellite-On-A-Chip." *Military & Aerospace Electronics*, Vol. 5(2), 1994, p. 1- 13.
3. Justin A. Atchison, Mason A. Peck, "A passive, sun-pointing, millimetre-scale solar sail," *Acta Astronautica* 67 (2010) 108–121
4. Barnhart, D. J., Vladimirova, T., and Sweeting, M.N. "Very-Small-Satellite Design for Distributed Space Missions." *J. of Spacecraft and Rockets*, Vol. 44(6), 2007, pp. 1294–1306.
5. Stuurman, B. and Kumar, K. "RyeFemSat: Ryerson University Femto-satellite Design and

- Testing,” in *Proc. of AIAA SpaceOps Conf.*, Huntsville, AL, 2010.
6. Tristanchio, J. and Gutierrez-Cabello, J. “A Probe of Concept for Femto-Satellites Based on Commercial-Off-the-Shelf,” in *Proc. of 30th IEEE/AIAA Digital Avionics Systems Conf.*, Seattle, WA, 2011, pp. 8A2–1–8A2–9.
 7. Atchison, J. A. and Peck, M. A. “Length Scaling in Spacecraft Dynamics.” *J. of Guidance, Control, and Dynamics*, Vol. 34(1), 2011, pp. 231–246.
 8. Z. Manchester, M. Peck, and A. Filo, “Kicksat: A crowd-funded mission to demonstrate the world’s smallest spacecraft,” AIAA/USU Conference on Small Satellites, 2013.
 9. Cao, J., Clemente, C., McInnes, C.R., Soraghan, J., and Uttamchandani, D.: “A novel concept for earth remote sensing using a bistatic femto-satellite swarm in sun synchronous orbit,” Paper IAC-15. B4.6B.4, International Astronautical Congress 2015, Jerusalem, 12-16 October 2015.